Structure elucidation of olanzapine molecular salts by combining mechanochemistry and MicroED

Diptajyoti Gogoi[a], Toshiyuki Sasaki*[b†], Takanori Nakane,[c] Akihiro Kawamoto,[c] Hironobu Hojo,[c] Genji Kurisu,*[c,d,e] Ranjit Thakuria*[a]

[a] Department of Chemistry, Gauhati University, Guwahati 781014, Assam, India. E-mail: ranjit.thakuria@gmail.com, ranjit.thakuria@gauhati.ac.in

[b] Department of Materials System Science, Yokohama City University; 22-2 Seto; Kanazawa-ku, Yokohama, Kanagawa 236-0027, Japan. E-mail: tsasaki@yokohama-cu.ac.jp

[c] Institute for Protein Research, Osaka University, 3-2 Yamadaoka, Suita, Osaka 565-0871, Japan.

[d] Department of Macromolecular Science, Graduate School of Science, Osaka University, Toyonaka 560-0043, Japan.

[e] Institute for Open and Transdisciplinary Research Initiatives, Osaka University, 2-1 Yamadaoka, Suita, Osaka 565-0871, Japan. Email: gkurisu@protein.osaka-u.ac.jp

Abstract

Olanzapine (OLN), an anti-psychotic drug, is one of the most widely studied pharmaceutical materials. Although OLN and most of their multicomponent solids are highly crystalline, some of their molecular salts are difficult to crystallize and optimization takes long time. After several batches of failed crystallization, we applied mechanochemistry and microcrystal electron diffraction (MicroED) for structure elucidation. This combined approach was successful not only in structure determination of the drug molecule but also in characterizing traces of impurity present in a bulk solid. This study demonstrates that the combined approach is fast and efficient for structure elucidation of pharmaceutical materials when generation of suitable single crystals is challenging.

Introduction

Structure elucidation of pharmaceutical material provides key insights in understanding molecular interactions and tuning physicochemical properties. Moreover, presence of molecular impurities such as polymorphs, decomposed products, starting materials or any forms of contaminant can

also alter the physicochemical property as well as the relative stability of the drug material.[1-3] Therefore, structural characterization of active pharmaceutical ingredients (APIs) as well as molecular impurities is of prime importance in pharmaceutical industry. It has been observed that most of the APIs or pharmaceutical multicomponent solids (salts, cocrystals, solvates, hydrates etc.) do not form suitable single crystals for structure elucidation by X-ray crystallography and optimization for structure determination takes long time.[4-6]

OLN is a well-known anti-psychotic drug, for which several polymorphs,[7,8] solvates,[9] cocrystals[10,11] and molecular salts[12,13] have been reported in the literature. It is one of the most widely studied psychoactive drug[14,15] and several publications have appeared from our research group as well.[4,7,12,13,16,17] In one of our previous works, we discussed the hydration stability of a series of OLN salts with aliphatic dicarboxylic acids.[4] During the investigation, although a few crystal structures were determined, we could not optimize the condition to generate suitable single crystals of olanzapinium oxalate, olanzapinium glutarate and olanzapinium succinate (Scheme 1). As an alternative, powder diffraction coupled with periodic DFT was used to determine the crystal structure of olanzapinium oxalate; however, we failed to do so for the other salts.

Advancement of electron diffraction techniques led to the development of microcrystal electron diffraction (MicroED), or continuous rotation electron crystallography, for structure solution of small molecules[18-25] as well as macromolecules like proteins and peptides.[26] MicroED can solve crystal structures from fine powders, even when it is a mixture of multiple compounds. Here, we applied MicroED and mechanochemistry to structure elucidation of pharmaceutical materials that failed to generate suitable single crystals by solution crystallization.

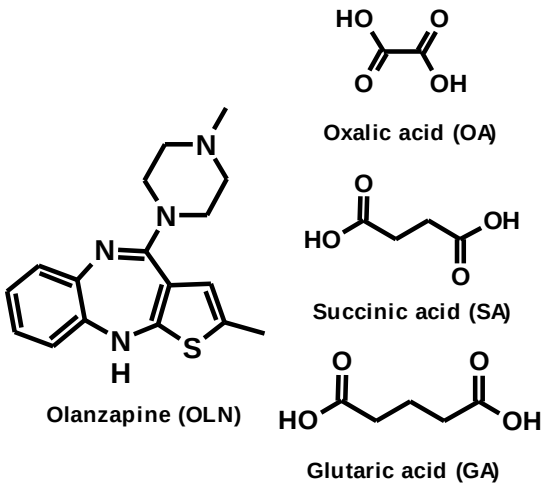

Scheme 1 Molecular structure of olanzapine (OLN) and salt formers oxalic acid (OA), succinic acid (SA) and glutaric acid (GA) considered for this study.

All the 1:1 molecular salts of OLN in powder form were prepared for MicroED using liquid assisted grinding (LAG) in the presence of acetonitrile as added liquid. The powdered molecular salts were gently dusted on a copper EM grid (Quantifoil R1.2/1.3 Cu 200 mech) and loaded onto a Talos Arctica microscope (Thermo Fisher Scientific) (Supporting information Figure S1). Data collection was performed on Talos Arctica operated at 200 kV using SerialEM[25] with a strategy described in the literature.[24,27,28] Briefly, crystals cryo-cooled to 79 K were rotated at 1 °/s for 60°, while the diffraction patterns were recorded on a Ceta detector at 1 frame/s. The electron flux is about 0.05 e/Å^{2}s. Diffraction patterns were processed with DIALS[29–31] and xia2.multiplex.[32] Merged intensities were phased by SHELXT[33] and kinematically refined with SHELXL[34] in Olex2 GUI.[35]

The first system, olanzapinium glutarate monohydrate (OLN^+•GA^-•H_2O) was characterized using SCXRD. During preparation of our previous report[4] (year 2018), after several batches of failed crystallization, we managed to generate olanzapinium glutarate acetonitrile salt that did not match the experimental PXRD patterns reported in that study. Although we proposed that mechanosynthesis resulted in olanzapinium glutarate monohydrate, based on thermal measurements, we could not determine its crystal structure. Accidently during co-crystallization of OLN with pyrazinamide for another work[17] (year 2020), a single crystal of the OLN^+•GA^-•H_2O was obtained along with the desired cocrystal. The crystal structure was solved in $P\bar{1}$ space group containing one molecule each of OLN^+, GA^- and water molecule in the asymmetric unit. One of the carboxylic acid protons of GA was transferred to the piperazine ring nitrogen of OLN resulting in the formation of a molecular salt. A water molecule connects the OLN^+ and GA^- dimer with N–H···O_{water} and O–H···O hydrogen bonds as shown in Figure 1a. 3D packing showed formation of OLN^+-GA^- infinite chains connected via N–H···O_{water}/N^+–H···O^- and O–H···O hydrogen bonds. Neighboring OLN molecules form an OLN dimer motif with C–H···π interactions (Figure 1b-c). The calculated powder pattern matches well with the experimental one confirming our earlier prediction.[4]

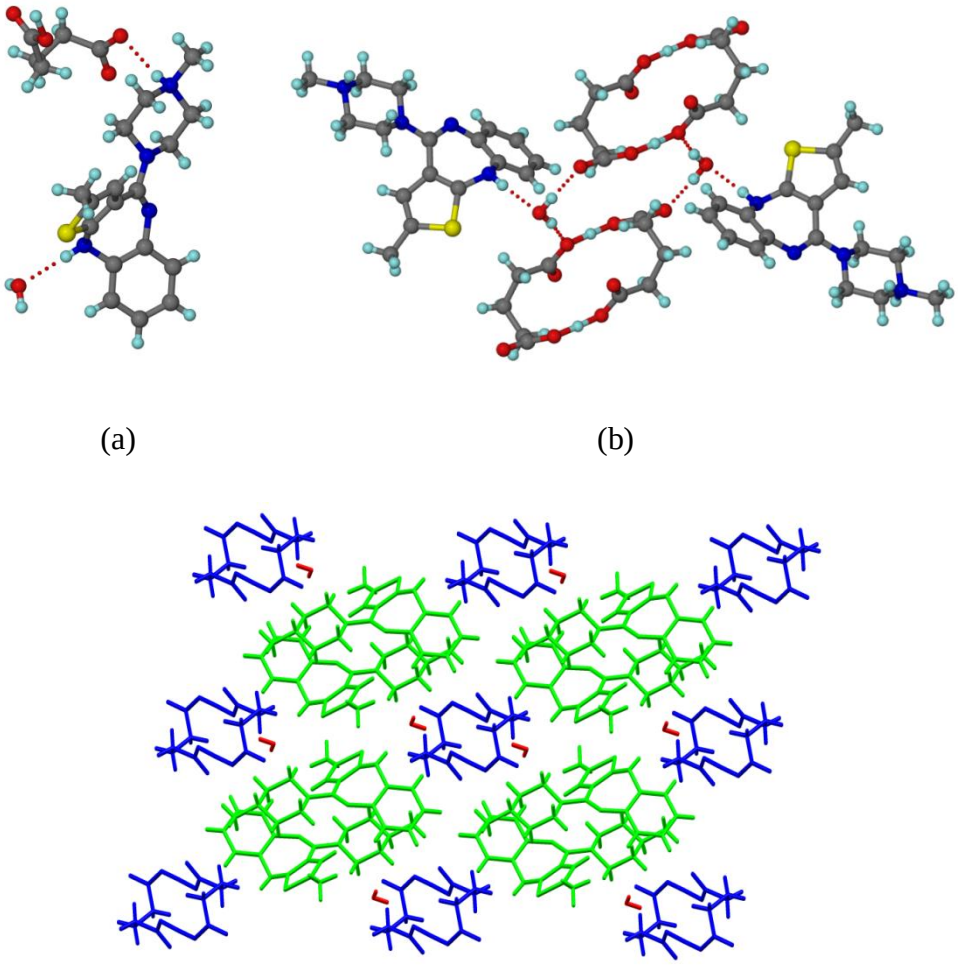

Figure 1 (a) OLN^{+} molecule connecting neighboring GA^{-} and water molecule using N^{+}–H···O^{-} and N–H···O_{water} hydrogen bond respectively; (b) Water molecule that acts as a bridge connecting GA^{-} dimers and OLN^{+} using N–H···O_{water} and O_{water}–H···O hydrogen bond; (c) 3D packing arrangement showing symmetry independent molecules with different color code.

The second system, crystal structure of olanzapinium oxalate (OLN^{2+}•OA^{2-}) was solved in the monoclinic chiral space group $P2_1$ using MicroED by merging 70 high-resolution crystals out of 247 measured, 204 indexed crystals. The crystal contained one molecule each of olanzapine and oxalic acid in the asymmetric unit. Two protons from the oxalic acid molecule were transferred to the piperazine and the diazapine ring nitrogens of OLN that resulted in a di-salt. The MicroED

structure showed cell parameters as well as crystal packing consistent with that of the reported[14] powder structure solution (Figure 2 and supporting information Table T1).

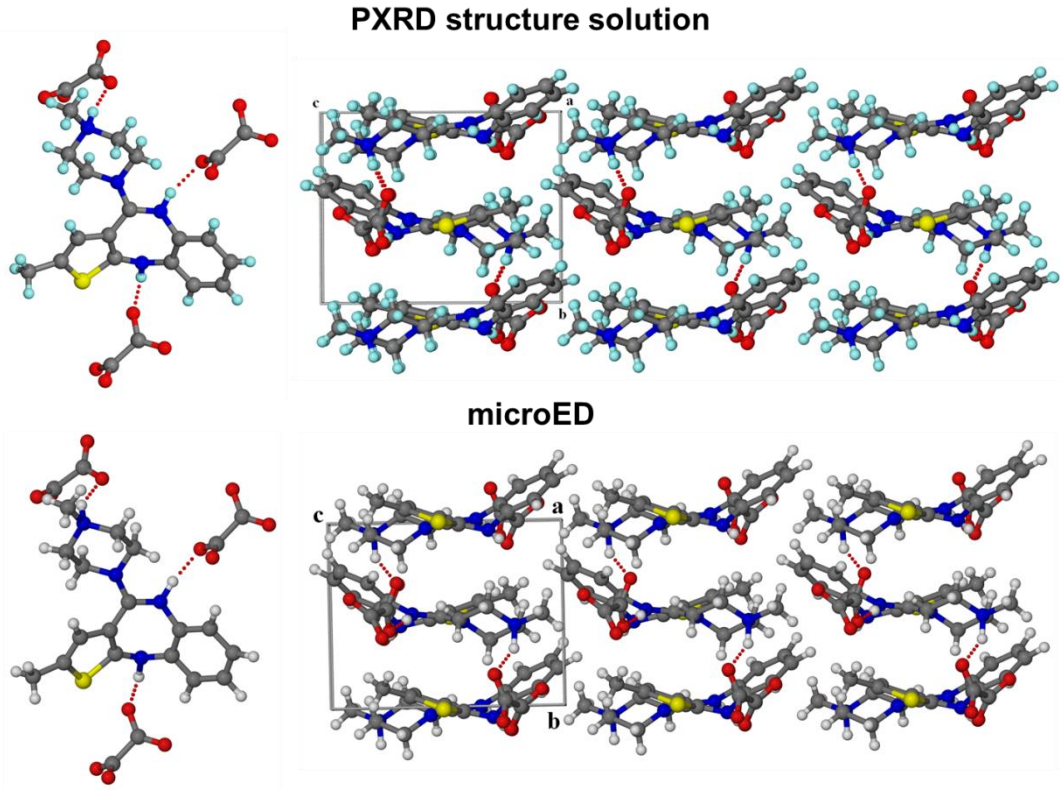

Figure 2 Hydrogen bond interactions and molecular packing pattern of OLN^{2+}•OA^{2-} salt solved using PXRD structure solution (reported) vs. MicroED (this study).

The third system, olanzapinium succinate molecular salt was analyzed with MicroED (Supporting information Figure S1). Indexing of 244 measured crystals gave at least three distinct unit cell parameters. 87 crystals were indexed in the most common crystal form. We merged 34 high-resolution crystals, which yielded the salt structure in the $P2_1/c$ space group containing one molecule each of OLN^+, SA^- and acetonitrile (ACN) in the asymmetric unit. Similar to all reported molecular salts, a proton is transferred from one of the carboxylic acid groups of SA to the piperazine ring nitrogen of OLN. The carboxylate oxygen has bifurcated interactions with two OLN molecules through the piperazine ring nitrogen and the diazapine ring N–H group using N^+–H···O^-_{SA} and N–H···O^-_{SA} hydrogen bonds, respectively. The second carboxylic acid group of SA forms a discrete hydrogen bond to the third OLN molecule via the diazapine ring nitrogen i.e. O–H···N, forming a 3D crystal packing arrangement as shown in Figure 3a. The void space is

occupied by an acetonitrile molecule forming a host-guest structure (Figure 3b). Crystallographic parameters of all the OLN salts considered in the study are summarized in the supporting information Table T1.

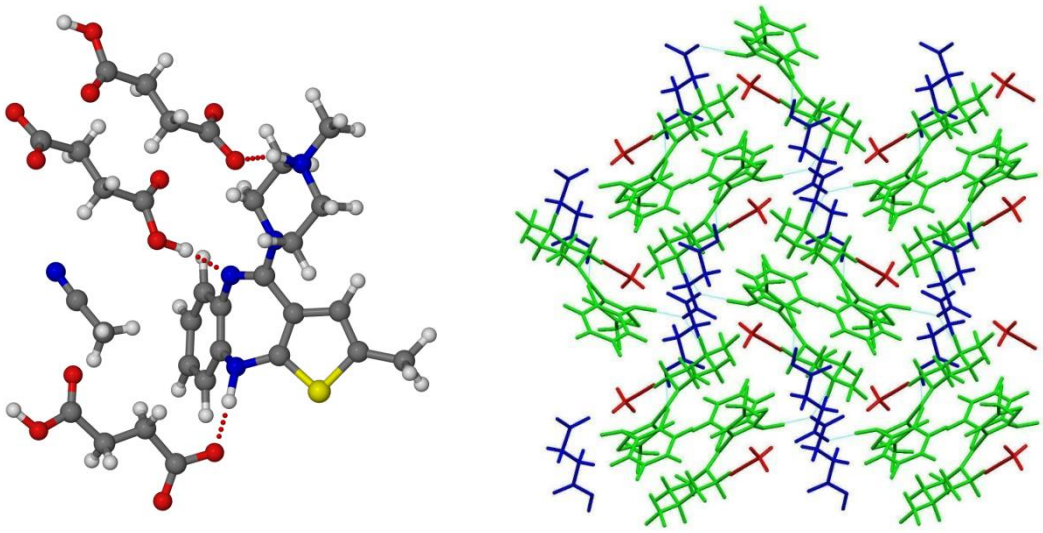

(a) (b)

Figure 3 (a) Various hydrogen bond interactions present between SA and OLN molecules in OLN^{+}•SA^{-}•ACN crystal structure; (b) Host-guest type of 3D packing arrangement with void space occupied by ACN solvent (red).

The calculated powder patterns of all the materials match well with their respective experimental powder patterns (Figure 4), confirming homogeneity (as less than 5% impurity is impossible to characterize using PXRD) of the powder sample as well as accurate structure solution of the investigated crystal systems.

During the MicroED structure determination of OLN^{+}•SA^{-}•ACN, we obtained two more structures; one contained an OLN fragment (28 merged out of 50 indexed), while the other was a 2:1:1 co-crystal of SUCA, 1-methylpiperadine and water (41 merged out of 68 indexed; see supporting information Figure S2-3 for structures). We surmise that these impurities were present in the sample before irradiation. First, the diffraction patterns indicated the unit cell parameters of impurity crystals from early frames; if the radiation damage had generated these impurities, the lattice would have started as that of OLN-SUCA and changed to that of impurity crystals towards later frames. Next, breakage of a C–N bond in OLN and its substitution to a C=O bond are unlikely,

especially at our low total electron flux of 3 e/Å^2. Although 1-methylpiperadine could result from OLN decomposition, the crystal packing of OLN-SUCA does not have void spaces to allow the remaining tricyclic ring to escape. Interestingly, however, ^{1}H- and ^{13}C-NMR spectra of the corresponding powder material did not show any impurity in the form of decomposed material (see supporting information Figure S4). Thus, we speculate that the sample contained these impurities at a trace amount during synthesis of the commercial drug[36] and below the detection limits of NMR and powder diffraction (< 5%). Note that the numbers of indexed crystals (87:50:68) do not reflect the composition in the bulk, because too large crystals and crystal aggregates cannot be measured and indexed in MicroED. The presence of the impurities before irradiation was confirmed by mass spectroscopy (MS). MS was measured after separating the impurity from the raw material (OLN powder) by HPLC (see supporting information Figure S5 for HPLC, TLC and MS data).

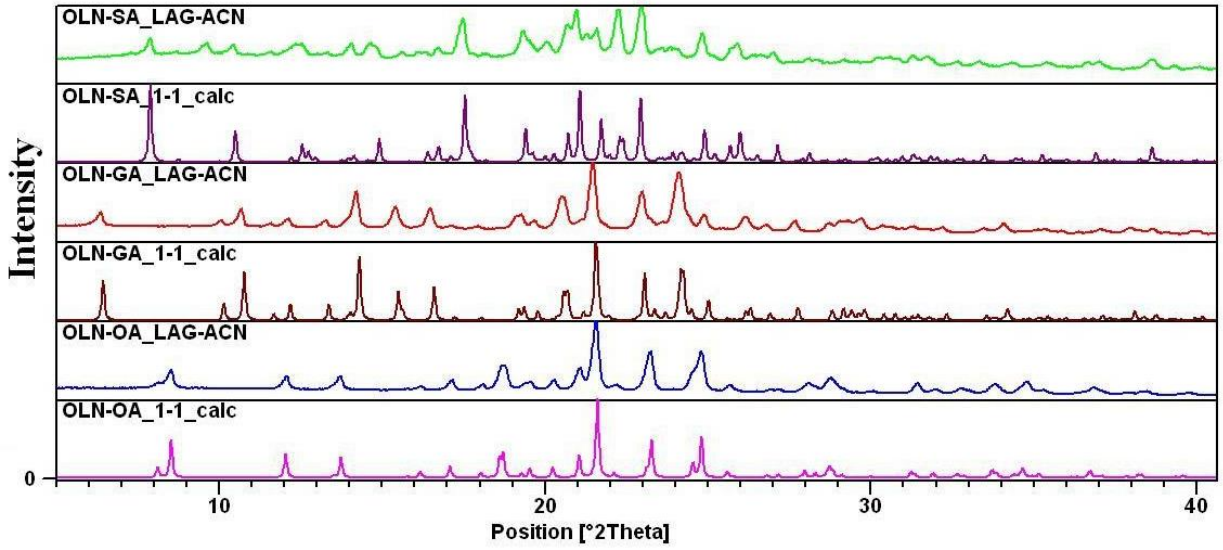

Figure 4 Comparison of experimental powder patterns with calculated powder patterns of OLN molecular salts considered for this study.

In conclusion, we successfully determined structures of olanzapine molecular salts: olanzapinium glutarate by SCXRD due to accidental formation of a suitable single crystal after 2 years from the first report[17], and olanzapinium oxalate and olanzapinium succinate directly from powdered samples by combination of mechanochemistry and MicroED. Although 2 years may not be a long period in academic settings to optimize crystallization, from an industrial point of view

it may fatally delay the launch of a potential drug candidate as a competitor may file a patent and enter into the market. Cumbersome and time-consuming optimization processes for generating single crystals suitable for structure determination by SCXRD were avoided by MicroED. It is also noteworthy that we succeeded in detecting and revealing structures of impurities by taking the basic advantage of MicroED, in which a large number of nanocrystals is individually located in the imaging mode and measured in the diffraction mode. Diffraction patterns from crystals are classified *in silico*, ameliorating the need to physically purify the mixture. Pharmaceutical industry will surely benefit from such advantages of combined mechanochemistry and MicroED in structure solution of APIs that are recalcitrant to yield large single crystals by traditional solution-phase crystallization.

Supporting Information

Cryo-EM images of OLN molecular salts, molecular structures of the OLN impurities, ^{1}H and ^{13}C-NMR spectra of OLN salts, crystallographic data table, HPLC, TLC and MS data of OLN impurities. CCDC No. 2254172-2254176. Raw diffraction images were deposited to XRDa (https://doi.org/10.51093/xrd-00125, https://doi.org/10.51093/xrd-00126).

Notes

The authors declare no competing financial interest.

Present address:

[†]T.S.: Japan Synchrotron Radiation Research Institute, 1-1-1 Kouto, Sayo-cho, Sayo-gun, Hyogo 679-5198, Japan

Email: toshiyuki.sasaki@spring8.or.jp

Acknowledgments

R.T. thanks the Science and Engineering Research Board for funding under the Teachers Associateship for Research Excellence (TARE) grant (Project No. TAR/2021/000251). R.T. thankfully acknowledge the Sophisticated Analytical Instrumentation Facility (SAIF), GU for the provision of the single crystal X-ray diffractometer and the Department of Chemistry, GU for the Rigaku powder X-ray diffractometer, basic instrumentation facility, and infrastructure. T.S. thanks JSPS KAKENHI Grant Number 22K05054 and Hitachi Metals-Materials Science Foundation.

This work was also supported by Research Support Project for Life Science and Drug Discovery (BINDS) from AMED under Grant Number JP22ama121001.

Reference

(1) Kras, W.; Carletta, A.; Montis, R.; Sullivan, R. A.; Cruz-Cabeza, A. J. Switching polymorph stabilities with impurities provides a thermodynamic route to benzamide form III. *Commun. Chem.*, **2021**, *4*, 1-7.

(2) Liu, Y.; Black, J. F. B.; Boon, K. F.; Cruz-Cabeza, A. J.; Davey, R. J.; Dowling, R. J.; George, N.; Hutchinson, A.; Montis, R. When Crystals Do Not Grow: The Growth Dead Zone. *Cryst. Growth Des.*, **2019**, *19*, 4579-4587.

(3) Chemburkar, S. R.; Bauer, J.; Deming, K.; Spiwek, H.; Patel, K.; Morris, J.; Henry, R.; Spanton, S.; Dziki, W.; Porter, W.; Quick, J.; Bauer, P.; Donaubauer, J.; Narayanan, B. A.; Soldani, M.; Riley, D.; McFarland, K. Dealing with the Impact of Ritonavir Polymorphs on the Late Stages of Bulk Drug Process Development. *Org. Process Res. Dev.*, **2000**, *4*, 413-417.

(4) Sarmah, K. K.; Sarma, P.; Rao, D. R.; Gupta, P.; Nath, N. K.; Arhangelskis, M.; Thakuria, R. Mechanochemical Synthesis of Olanzapine Salts and Their Hydration Stability Study Using Powder X-ray Diffraction. *Cryst. Growth Des.*, **2018**, *18*, 2138-2150.

(5) Surov, A. O.; Voronin, A. P.; Manin, A. N.; Manin, N. G.; Kuzmina, L. G.; Churakov, A. V.; Perlovich, G. L. Pharmaceutical Cocrystals of Diflunisal and Diclofenac with Theophylline. *Mol. Pharm.*, **2014**, *11*, 3707-3715.

(6) Grecu, T.; Prohens, R.; McCabe, J. F.; Carrington, E. J.; Wright, J. S.; Brammer, L.; Hunter, C. A. Cocrystals of spironolactone and griseofulvin based on an in silico screening method. *CrystEngComm* **2017**, *19*, 3592-3599.

(7) Thakuria, R.; Nangia, A. Polymorphic form IV of olanzapine. *Acta crystallogr., C: Cryst. Struct. Commun.*, **2011**, *67*, o461-o463.

(8) Askin, S.; Cockcroft, J. K.; Price, L. S.; Gonçalves, A. D.; Zhao, M.; Tocher, D. A.; Williams, G. R.; Gaisford, S.; Craig, D. Q. M. Olanzapine Form IV: Discovery of a New Polymorphic Form Enabled by Computed Crystal Energy Landscapes. *Cryst. Growth Des.*, **2019**, *19*, 2751-2757.

(9) Reutzel-Edens, S. M.; Bush, J. K.; Magee, P. A.; Stephenson, G. A.; Byrn, S. R. Anhydrates and Hydrates of Olanzapine: Crystallization, Solid-State Characterization, and Structural Relationships. *Cryst. Growth Des.*, **2003**, *3*, 897-907.

(10) Andrusenko, I.; Potticary, J.; Hall, S. R.; Gemmi, M. A new olanzapine cocrystal obtained from volatile deep eutectic solvents and determined by 3D electron diffraction. *Acta. Crystallogr. B: Struct. Sci. Cryst. Eng. Mater.*, **2020**, *76*, 1036-1044.

(11) Surampudi, A. V. S. D.; Rajendrakumar, S.; Nanubolu, J. B.; Balasubramanian, S.; Surov, A. O.; Voronin, A. P.; Perlovich, G. L. Influence of crystal packing on the thermal properties of cocrystals and cocrystal solvates of olanzapine: insights from computations. *CrystEngComm* **2020**, *22*, 6536-6558.

(12) Thakuria, R.; Nangia, A. Olanzapinium Salts, Isostructural Solvates, and Their Physicochemical Properties. *Cryst. Growth Des.*, **2013**, *13*, 3672-3680.

(13) Sarmah, K. K.; Sarma, A.; Roy, K.; Rao, D. R.; Thakuria, R. Olanzapine Salts and Diversity in Molecular Packing. *Cryst. Growth Des.*, **2016**, *16*, 1047-1055.

(14) Bhardwaj, R. M.; Price, L. S.; Price, S. L.; Reutzel-Edens, S. M.; Miller, G. J.; Oswald, I. D. H.; Johnston, B. F.; Florence, A. J. Exploring the Experimental and Computed Crystal Energy Landscape of Olanzapine. *Cryst. Growth Des.,* **2013**, *13*, 1602-1617.

(15) Reutzel-Edens, S. M.; Bhardwaj, R. M. Crystal forms in pharmaceutical applications: olanzapine, a gift to crystal chemistry that keeps on giving. *IUCrJ* **2020**, *7*, 955-964.

(16) Thakuria, R.; Nangia, A. Highly soluble olanzapinium maleate crystalline salts. *CrystEngComm* **2011**, *13*, 1759-1764.

(17) Sarmah, K. K.; Nath, N.; Rao, D. R.; Thakuria, R. Mechanochemical synthesis of drug–drug and drug–nutraceutical multicomponent solids of olanzapine. *CrystEngComm* **2020**, *22*, 1120-1130.

(18) Gruene, T.; Wennmacher, J. T. C.; Zaubitzer, C.; Holstein, J. J.; Heidler, J.; Fecteau-Lefebvre, A.; De Carlo, S.; Müller, E.; Goldie, K. N.; Regeni, I.; Li, T.; Santiso-Quinones, G.; Steinfeld, G.; Handschin, S.; van Genderen, E.; van Bokhoven, J. A.; Clever, G. H.; Pantelic, R. Rapid Structure Determination of Microcrystalline Molecular Compounds Using Electron Diffraction. *Angew. Chem. Int. Ed.*, **2018**, *57*, 16313-16317.

(19) Ito, S.; White, F. J.; Okunishi, E.; Aoyama, Y.; Yamano, A.; Sato, H.; Ferrara, J. D.; Jasnowski, M.; Meyer, M. Structure determination of small molecule compounds by an electron diffractometer for 3D ED/MicroED. *CrystEngComm* **2021**, *23*, 8622-8630.

(20) Jones, C. G.; Martynowycz, M. W.; Hattne, J.; Fulton, T. J.; Stoltz, B. M.; Rodriguez, J. A.; Nelson, H. M.; Gonen, T. The CryoEM Method MicroED as a Powerful Tool for Small Molecule Structure Determination. *ACS Cent. Sci.*, **2018**, *4*, 1587-1592.

(21) Newman, J. A.; Iuzzolino, L.; Tan, M.; Orth, P.; Bruhn, J.; Lee, A. Y. From Powders to Single Crystals: A Crystallographer's Toolbox for Small-Molecule Structure Determination. *Mol. Pharm.*, **2022**, *19*, 2133-2141.

(22) Lightowler, M.; Li, S.; Ou, X.; Zou, X.; Lu, M.; Xu, H. Indomethacin Polymorph δ Revealed To Be Two Plastically Bendable Crystal Forms by 3D Electron Diffraction: Correcting a 47-Year-Old Misunderstanding. *Angew. Chem. Int. Ed.*, **2022**, *61*, e202114985.

(23) Hitchen, J.; Andrusenko, I.; Hall, C. L.; Mugnaioli, E.; Potticary, J.; Gemmi, M.; Hall, S. R. Organic Cocrystals of TCNQ and TCNB Based on an Orthocetamol Backbone Solved by Three-Dimensional Electron Diffraction. *Cryst. Growth Des.,* **2022**, *22*, 1155-1163.

(24) Sasaki, T.; Nakane, T.; Kawamoto, A.; Nishizawa, T.; Kurisu, G. Microcrystal Electron Diffraction (MicroED) Structure Determination of a Mechanochemically Synthesized Co-crystal not Affordable from Solution Crystallization. *CrystEngComm* **2023**, *25*, 352-356.

(25) Smalley, C. J. H.; Hoskyns, H. E.; Hughes, C. E.; Johnstone, D. N.; Willhammar, T.; Young, M. T.; Pickard, C. J.; Logsdail, A. J.; Midgley, P. A.; Harris, K. D. M. A structure determination protocol based on combined analysis of 3D-ED data, powder XRD data, solid-state NMR data and DFT-D calculations reveals the structure of a new polymorph of l-tyrosine. *Chem. Sci.,* **2022**, *13*, 5277-5288.

(26) Saha, A.; Nia, S. S.; Rodríguez, J. A. Electron Diffraction of 3D Molecular Crystals. *Chem. Rev.,* **2022**, *122*, 13883-13914.

(27) Hamada, H.; Nakamuro, T.; Yamashita, K.; Yanagisawa, H.; Nureki, O.; Kikkawa, M.; Harano, K.; Shang, R.; Nakamura, E. Spiro-Conjugated Carbon/Heteroatom-Bridged p-Phenylenevinylenes: Synthesis, Properties, and Microcrystal Electron Crystallographic Analysis of Racemic Solid Solutions. *Bull. Chem. Soc. Jpn.*, **2020**, *93*, 776-782.

(28) Lu, H.; Nakamuro, T.; Yamashita, K.; Yanagisawa, H.; Nureki, O.; Kikkawa, M.; Gao, H.; Tian, J.; Shang, R.; Nakamura, E. B/N-Doped p-Arylenevinylene Chromophores:

Synthesis, Properties, and Microcrystal Electron Crystallographic Study. *J. Am. Chem. Soc.*, **2020**, *142*, 18990-18996.

(29) Winter, G.; Waterman, D. G.; Parkhurst, J. M.; Brewster, A. S.; Gildea, R. J.; Gerstel, M.; Fuentes-Montero, L.; Vollmar, M.; Michels-Clark, T.; Young, I. D.; Sauter, N. K.; Evans, G. DIALS: implementation and evaluation of a new integration package. *Acta Cryst.*, **2018**, *D74*, 85–97.

(30) Clabbers, M. T. B.; Gruene, T.; Parkhurst, J. M.; Abrahams, J. P.; Waterman, D. G. Electron diffraction data processing with DIALS. *Acta Cryst.*, **2018**, *D74*, 506–518.

(31) Beilsten-Edmands, J.; Winter, G.; Gildea, R.; Parkhurst, J.; Waterman, D.; Evans, G. Scaling diffraction data in the DIALS software package: algorithms and new approaches for multi-crystal scaling. *Acta Cryst.*, **2020**, *D76*, 385–399.

(32) Gildea, R. J.; Beilsten-Edmands, J.; Axford, D.; Horrell, S.; Aller, P.; Sandy, J.; Sanchez-Weatherby, J.; Owen, C. D.; Lukacik, P.; Strain-Damerell, C.; Owen, R. L.; Walsh, M. A.; Winter, G. xia2.multiplex: a multi-crystal data-analysis pipeline, *Acta Cryst.*, **2022**, *D78*, 752–769.

(33) Sheldrick, G. M. SHELXT - Integrated space-group and crystal-structure determination. *Acta Cryst.*, **2015**, *A71*, 3–8.

(34) Sheldrick, G. M. Crystal structure refinement with SHELXL. *Acta Cryst.*, **2015**, *C71*, 3–8.

(35) Dolomanov, O. V.; Bourhis, L. J.; Gildea, R. J.; Howard, J. A. K.; Puschmann, H. OLEX2: a complete structure solution, refinement and analysis program. *J. Appl. Cryst.*, **2009**, *42*, 339–341.

(36) Cui, D.; Li, Y.; Lian, M.; Yang, F.; Meng, Q. Development of a simple and stability-indicating RP-HPLC method for determining olanzapine and related impurities generated in the preparative process. *Analyst*, **2011**, *136*, 3149-3156.

Supporting Information file

Structure elucidation of olanzapine molecular salts by combining mechanochemistry and MicroED

Diptajyoti Gogoi[a], Toshiyuki Sasaki*[b†], Takanori Nakane,[c] Akihiro Kawamoto,[c] Hironobu Hojo,[c] Genji Kurisu,*[c,d,e] Ranjit Thakuria*[a]

[a] Department of Chemistry, Gauhati University, Guwahati 781014, Assam, India. E-mail: ranjit.thakuria@gmail.com, ranjit.thakuria@gauhati.ac.in

[b] Department of Materials System Science, Yokohama City University; 22-2 Seto; Kanazawa-ku, Yokohama, Kanagawa 236-0027, Japan. E-mail: tsasaki@yokohama-cu.ac.jp

[c] Institute for Protein Research, Osaka University, 3-2 Yamadaoka, Suita, Osaka 565-0871, Japan.

[d] Department of Macromolecular Science, Graduate School of Science, Osaka University, Toyonaka 560-0043, Japan.

[e] Institute for Open and Transdisciplinary Research Initiatives, Osaka University, 2-1 Yamadaoka, Suita, Osaka 565-0871, Japan. Email: gkurisu@protein.osaka-u.ac.jp

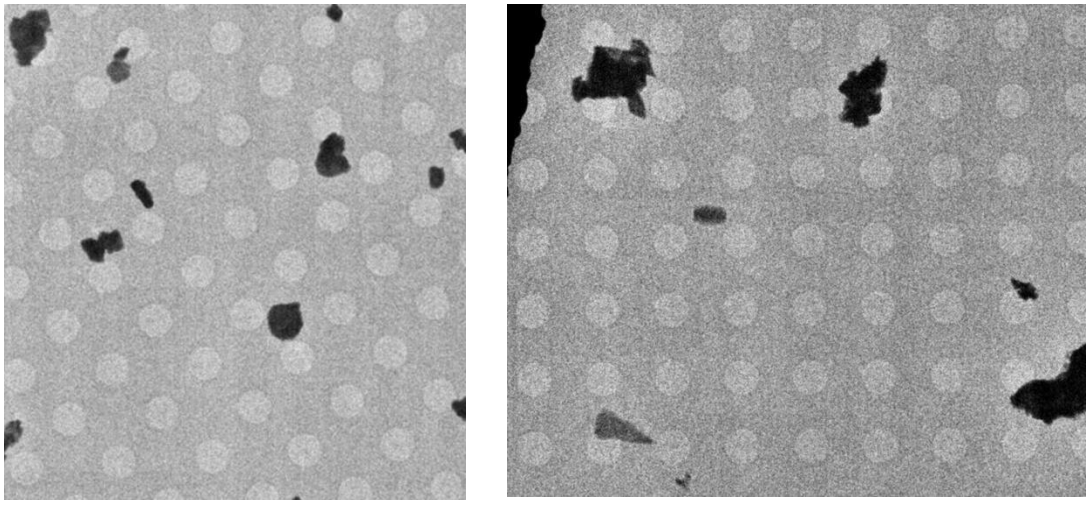

(a) (b)

Figure S1. Cryo-EM images of (a) OLN-OA and (b) OLN-SA powder prepared using manual grinding mounted on a copper EM grid for MicroED. (Scale: Diameter of circles in the photos is ca. 1.2 um)

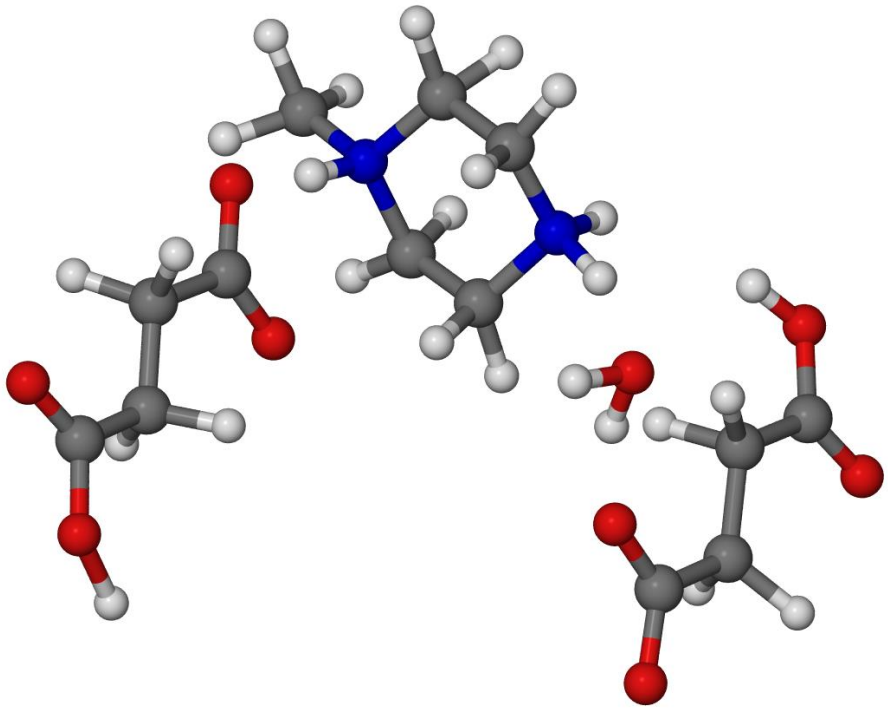

Figure S2. Molecules present in the asymmetric unit of one of the impurities of OLN-SA sample (impurity 1) used for MicroED analysis.

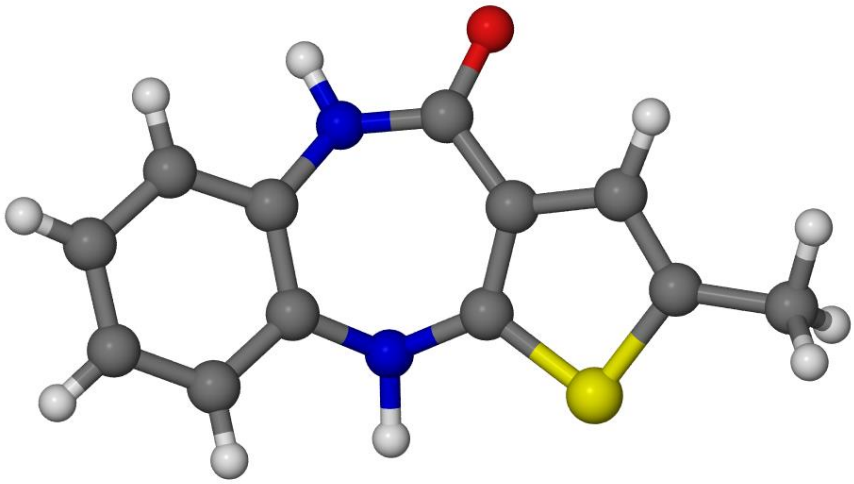

Figure S3. Molecules present in the asymmetric unit of the other impurity (impurity 2) of OLN-SA sample used for MicroED analysis.

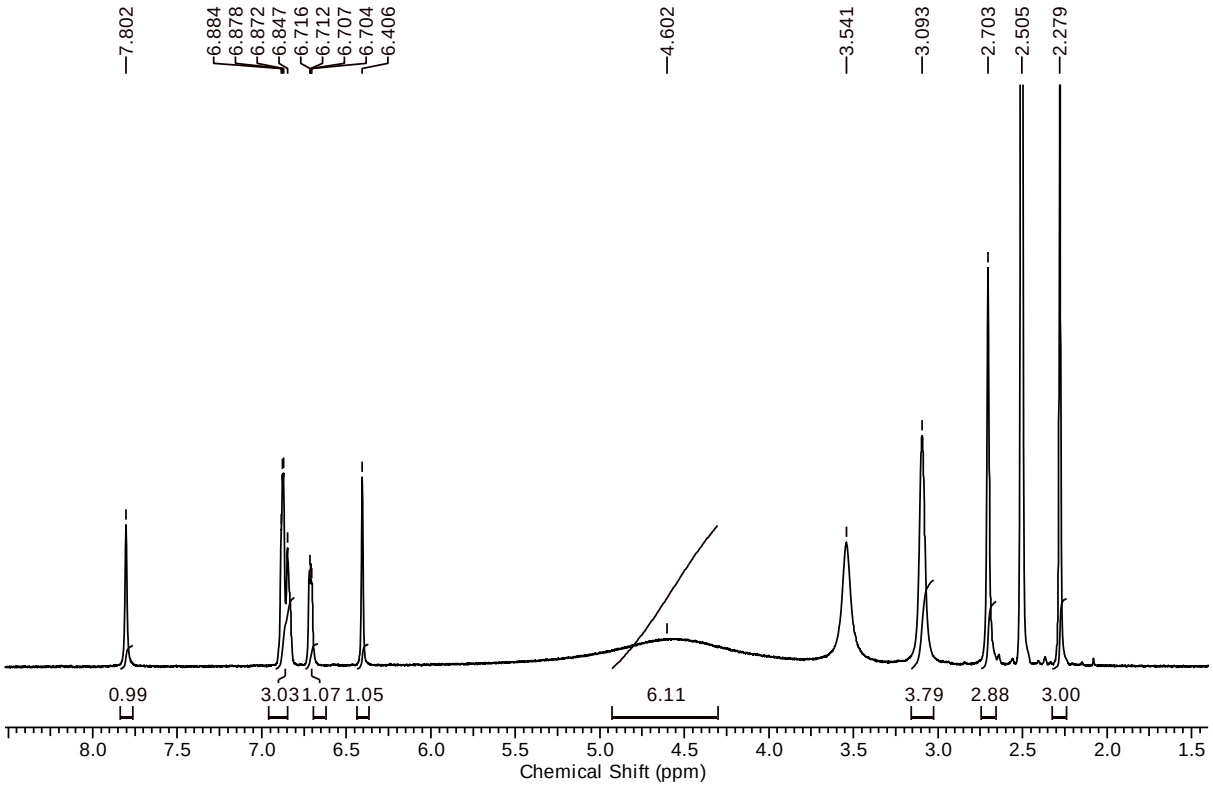

OLN^{2+}•OA^{2-}:

^{1}H NMR (DMSO-d_6, 400 MHz) δ: 7.80 (s, 1H), 6.88-6.84 (m, 3H), 6.71-6.70 (m, 1H), 6.40 (s, 1H), 4.60 (br, 6H), 3.09 (s, 4H), 2.70 (s, 3H), 2.27 (s, 3H) ppm.

(a)

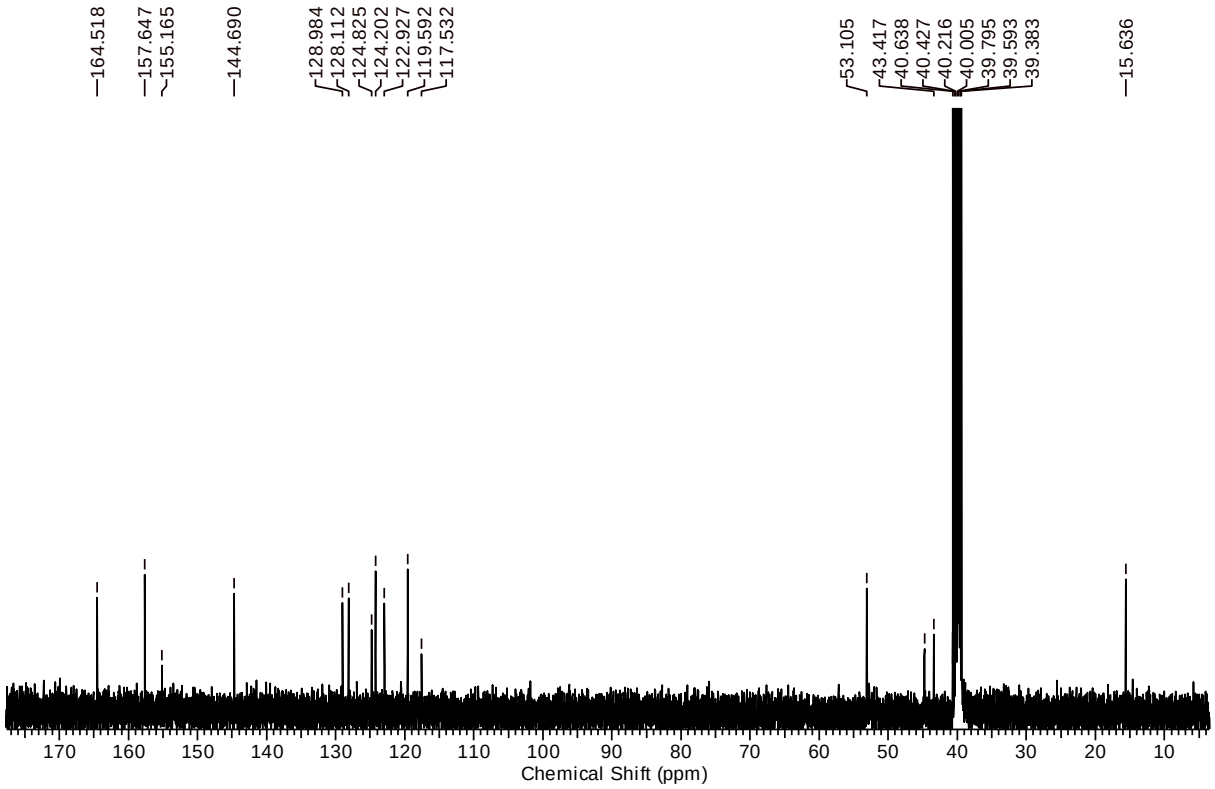

OLN^{2+}•OA^{2-}:

^{13}C NMR (DMSO-d_6, 100 MHz) δ: 164.5, 157.6, 155.1, 144.6, 128.9, 128.1, 124.8, 124.2, 122.9, 119.5, 117.5, 53.1, 44.7, 43.4, 15.6 ppm.

(b)

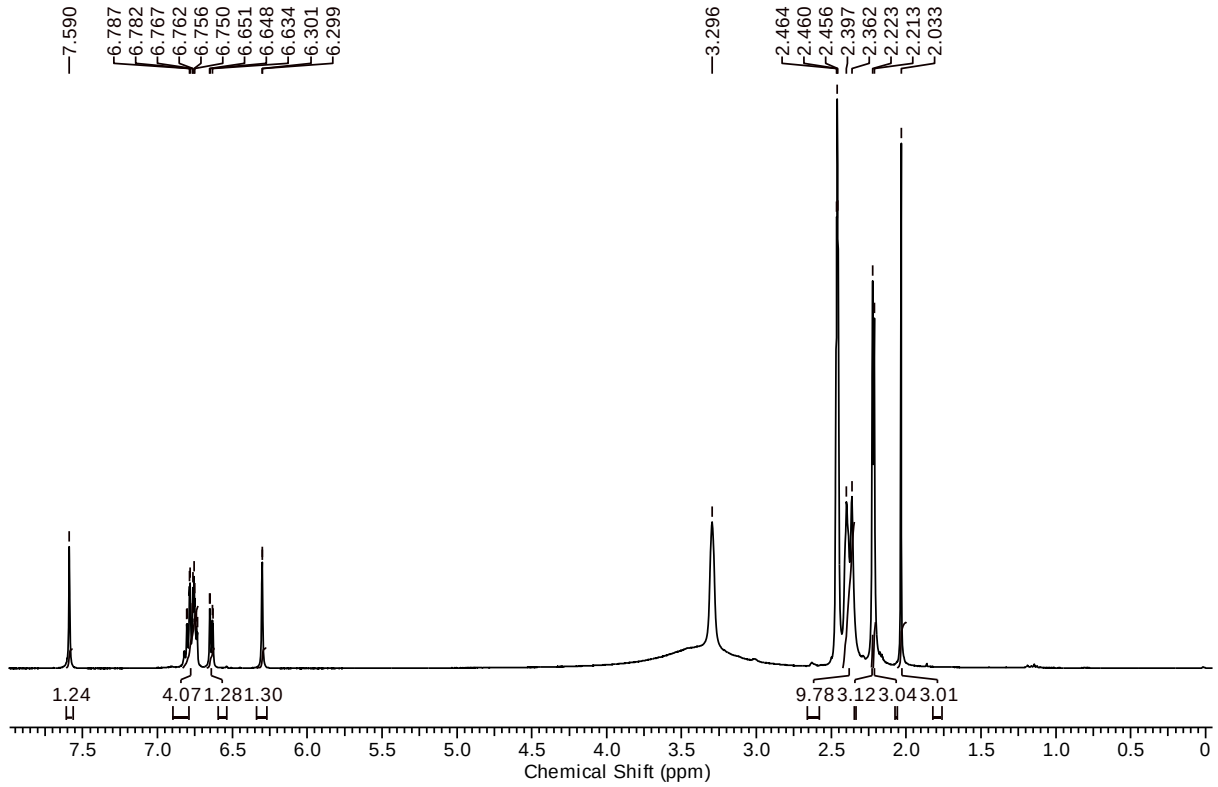

$OLN^{+}•SA^{-}$:

^{1}H NMR (DMSO-d_6, 400 MHz) δ: 7.59 (s, 1H), 6.80-6.73 (m, 4H), 6.65-6.62 (m, 1H), 6.30 (s, 1H), 2.37 (d, J = 14 Hz, 10H), 2.22 (s, 3H), 2.21 (s, 3H), 2.03 (s, 3H) ppm.

(c)

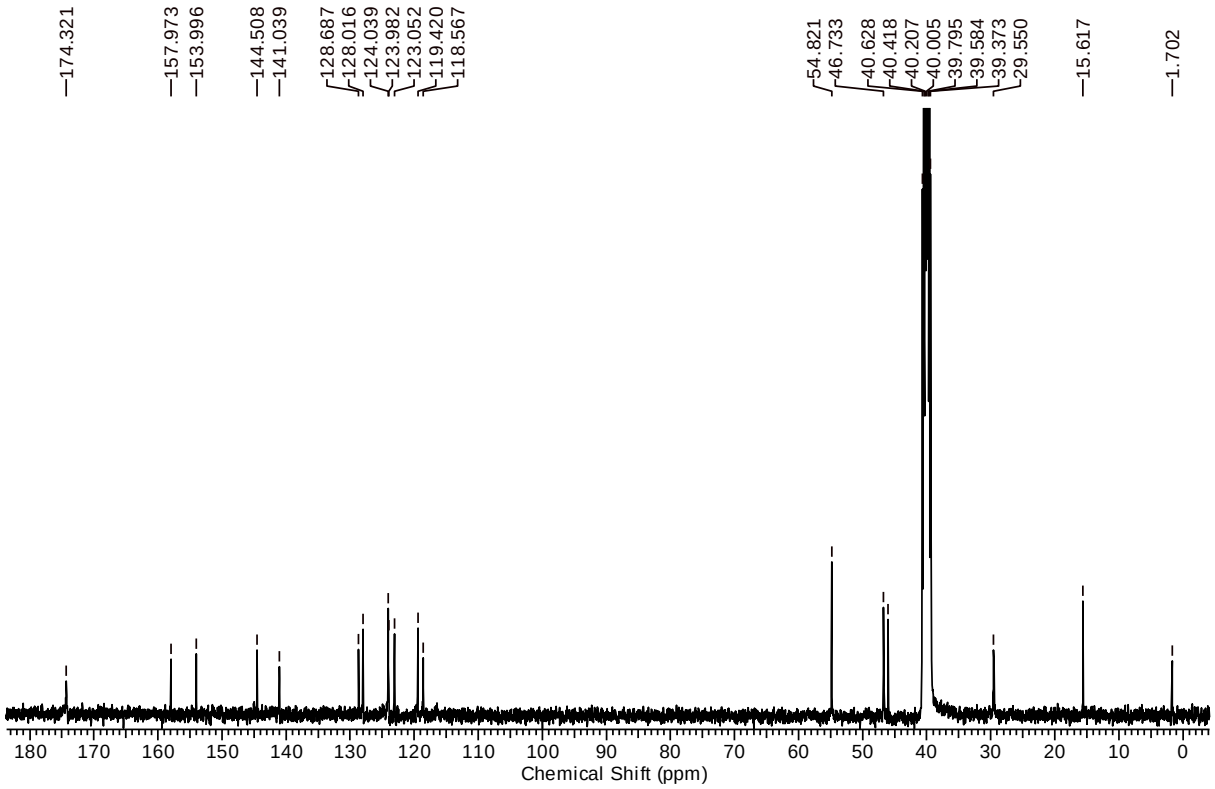

$OLN^{+}•SA^{-}$:

^{13}C NMR (DMSO-d_6, 100 MHz) δ: 174.3, 157.9, 153.9, 144.5, 141.0, 128.6, 128.0, 124.0, 123.0, 119.4, 118.5, 54.8, 46.7, 46.0, 29.5, 15.6, 1.7 ppm.

(d)

Figure S4. ^{1}H- and ^{13}C-NMR spectra of the corresponding (a-b) $OLN^{2+}•OA^{2-}$ and (c-d) $OLN^{+}•SA^{-}$ salt structures respectively.

Table T1. Crystallographic parameters of OLN salts

	Olanzapinium oxalate (1:1) (reported)	**Olanzapinium oxalate (1:1) (this study)**	**Olanzapinium glutarate monohydrate (1:1:1)**	**Olanzapinium succinate acetonitrile (1:1:1)**	**Olanzapine impurity 1 (2:1:1)**	**Olanzapine impurity 2**
Chemical formula	$(C_{17}H_{22}N_4S)•(C_2O_4)$	$(C_{17}H_{22}N_4S)•(C_2O_4)$	$(C_{17}H_{21}N_4S)•0.5(C_{10}H_{14}O_8)•H_2O$	$(C_{17}H_{22}N_4S)•(C_4H_5O_4)•(C_2H_3N)$	$2(C_4H_5O_4)•(C_5H_{14}N_2)•(H_2O)$	$(C_{12}H_{10}N_2OS)$
Formula wt	402.47	402.48	462.56	471.57	354.35	230.29
Cryst syst	Monolinic	Monoclinic	Triclinic	Monoclinic	Triclinic	Orthorhombic

Space group	$P2_1$	$P2_1$	$P\bar{1}$	$P2_1/c$	$P\bar{1}$	*Pbcn*
T, K	298	79	296	79	79	79
a, Å	10.3247(10)	10.914	8.3239(4)	11.718	6.605	10.815
b, Å	8.2245(5)	8.223	9.8354(5)	14.498	8.935	12.611
c, Å	10.8567(7)	10.386	14.1883(7)	14.742	15.061	16.549
α, deg	90	90	78.613(2)	90	104.04	90
β, deg	92.685(6)	87.44	80.880(3)	106.84	97.60	90
γ, deg	90	90	87.127(3)	90	97.50	90
Z	2	2	2	2	1	4
V, $Å^3$	920.88(12)	931.2	1124.11(10)	2397.1	842.2	2257.1
Dcalc, g cm^{-3}	1.452	1.435	1.367	1.307	1.397	1.355
μ, mm^{-1}	-	-	0.19	-	-	-
reflns collected	-	198554	4661	93754	45547	94540
unique reflns	-	5651	3836	4069	3004	2309
R1[I > 2(I)]	-	0.1097	0.042	0.1565	0.148	0.138
wR2 (all)	-	0.1371	0.127	0.1942	0.420	0.349
R_{wp} (powder data)	0.056	-	-	-	-	-
GOF	8.546	1.096	1.10	1.095	1.20	1.21
Data collection	Rigaku Ultima IV	Talos Arctica microscope	Bruker APEX-II CCD diffractometer	Talos Arctica microscope	Talos Arctica microscope	Talos Arctica microscope
CCDC no.	1585240	2254175	2254176	2254174	2254172	2254173

Table T2. Merging statistics of olanzapinium oxalate (1:1) solved by MicroED

d_max	d_min	#obs	#uniq	mult.	%comp	<I>	<I/sI>	r_mrg	r_means	r_pim	cc1/2
5.62	1.88	7747	165	46.95	98.21	3.6	85.4	0.16	0.162	0.022	0.997*
1.88	1.5	9188	154	59.66	100	1.8	47.5	0.256	0.259	0.033	0.996*
1.5	1.31	10128	157	64.51	100	1.2	32.9	0.339	0.342	0.041	0.984*
1.31	1.19	9662	153	63.15	100	1.2	28.5	0.337	0.34	0.042	0.993*
1.19	1.11	9832	152	64.68	100	1	22.3	0.447	0.451	0.054	0.973*
1.11	1.04	9611	146	65.83	100	0.8	19.9	0.425	0.429	0.052	0.981*
1.04	0.99	10057	155	64.88	100	0.6	13.6	0.552	0.557	0.067	0.979*
0.99	0.95	10958	154	71.16	100	0.4	11.2	0.688	0.693	0.082	0.945*
0.95	0.91	8790	144	61.04	100	0.3	7.2	1.041	1.049	0.126	0.867*
0.91	0.88	11654	157	74.23	100	0.3	7.3	1.075	1.082	0.123	0.899*
0.88	0.85	9600	149	64.43	100	0.2	5.3	1.247	1.256	0.15	0.890*
0.85	0.83	9433	140	67.38	100	0.2	4.8	1.354	1.365	0.165	0.856*
0.83	0.81	10586	153	69.19	100	0.1	3.6	1.574	1.585	0.185	0.806*
0.81	0.79	10389	151	68.8	100	0.1	3.5	1.807	1.82	0.212	0.721*
0.79	0.77	10427	151	69.05	100	0.1	3	1.989	2.005	0.242	0.747*
0.77	0.75	9800	152	64.47	100	0.1	2.5	2.167	2.185	0.269	0.634*
0.75	0.74	10200	137	74.45	100	0.1	2.2	3.567	3.592	0.412	0.363*
0.74	0.73	10254	154	66.58	100	0.1	1.8	3.1	3.124	0.376	0.556*
0.73	0.71	11541	165	69.95	100	0.1	1.6	3.23	3.253	0.373	0.433*
0.71	0.7	9026	118	76.49	100	0.1	1.7	11.973	12.055	1.368	0.435*
5.62	0.7	198883	3007	66.14	99.9	0.6	15.8	0.549	0.553	0.067	0.996*

Table T3. Merging statistics of olanzapinium succinate acetonitrile (1:1:1) solved by MicroED

d_max	d_min	#obs	#uniq	mult.	%comp	<I>	<I/sI>	r_mrg	r_means	r_pim	cc1/2
5.82	2.14	4204	269	15.63	100	1.5	34	0.312	0.321	0.076	0.995*
2.14	1.71	5481	263	20.84	100	0.8	20.8	0.504	0.515	0.107	0.992*

1.71	1.5	5624	256	21.97	100	0.5	13.7	0.704	0.719	0.146	0.983*
1.5	1.36	5850	261	22.41	100	0.3	9.2	0.803	0.821	0.172	0.961*
1.36	1.27	5774	257	22.47	100	0.4	9.3	0.76	0.778	0.164	0.974*
1.27	1.19	5738	253	22.68	100	0.3	7.8	0.838	0.857	0.179	0.971*
1.19	1.13	5845	250	23.38	100	0.3	7.8	0.956	0.976	0.195	0.978*
1.13	1.08	5890	258	22.83	100	0.2	5.6	0.939	0.96	0.197	0.975*
1.08	1.04	5897	252	23.4	100	0.2	5	1.026	1.047	0.211	0.945*
1.04	1.01	6203	264	23.5	100	0.2	3.8	1.006	1.027	0.202	0.924*
1.01	0.98	5563	234	23.77	100	0.1	2.9	1.14	1.166	0.238	0.889*
0.98	0.95	6082	260	23.39	100	0.1	2.3	1.308	1.335	0.263	0.902*
0.95	0.92	6033	253	23.85	100	0.1	2.1	1.6	1.634	0.325	0.854*
0.92	0.9	5679	243	23.37	100	0.1	1.8	1.212	1.237	0.248	0.816*
0.9	0.88	6399	269	23.79	100	0.1	1.6	1.71	1.745	0.343	0.831*
0.88	0.86	5723	238	24.05	100	0.1	1.4	1.565	1.596	0.314	0.573*
0.86	0.84	6063	255	23.78	100	0	1.1	1.415	1.444	0.286	0.666*
0.84	0.83	6059	257	23.58	100	0	1	1.676	1.711	0.345	0.753*
0.83	0.81	6100	255	23.92	100	0	1	1.734	1.772	0.365	0.549*
0.81	0.8	5130	245	20.94	100	0	0.8	2.416	2.474	0.524	0.560*
5.82	0.8	115337	5092	22.65	100	0.3	6.8	0.943	0.963	0.196	0.993*

Table T4. Merging statistics of one of the impurities in olanzapinium succinate (1:1) solved by MicroED

d_max	d_min	#obs	#uniq	mult.	%comp	<I>	<I/sI>	r_mrg	r_means	r_pim	cc1/2
5.63	2.13	1664	144	11.56	83.24	11	22.5	0.117	0.123	0.033	0.990*
2.13	1.71	2074	143	14.5	85.63	5.6	15.7	0.164	0.169	0.04	0.987*
1.71	1.5	2209	152	14.53	89.41	3.2	10.8	0.229	0.236	0.054	0.983*
1.5	1.36	2415	156	15.48	88.14	2.3	9.5	0.291	0.3	0.068	0.980*
1.36	1.27	2215	144	15.38	85.71	2.2	8.5	0.277	0.286	0.067	0.989*
1.27	1.19	2597	155	16.75	88.57	2.2	8.6	0.24	0.246	0.051	0.995*
1.19	1.13	1866	143	13.05	87.73	1.4	5.4	0.3	0.311	0.073	0.975*

1.13	1.08	2484	159	15.62	89.33	1.4	5.5	0.343	0.353	0.079	0.984*
1.08	1.04	2594	155	16.74	87.57	1.1	5.2	0.407	0.418	0.09	0.964*
1.04	1.01	2319	151	15.36	88.3	0.9	4.4	0.426	0.438	0.096	0.964*
1.01	0.98	2275	145	15.69	87.35	0.6	3.3	0.469	0.486	0.111	0.458*
0.98	0.95	1949	139	14.02	85.8	0.5	2.4	0.558	0.577	0.137	0.904*
0.95	0.92	2779	168	16.54	90.81	0.5	2.8	0.667	0.685	0.146	0.810*
0.92	0.9	2282	149	15.32	86.13	0.3	1.5	1.056	1.089	0.247	0.693*
0.9	0.88	2497	154	16.21	88	0.3	1.5	0.926	0.951	0.202	0.790*
0.88	0.86	2258	144	15.68	88.34	0.1	1.2	1.093	1.127	0.252	0.220*
0.86	0.84	2342	156	15.01	87.64	0.2	1	1.291	1.329	0.291	0.663*
0.84	0.83	1998	137	14.58	87.82	0.2	1.2	1.084	1.133	0.29	-0.105
0.83	0.81	2597	161	16.13	88.46	0.2	1.1	1.727	1.792	0.412	-0.449
0.81	0.8	2137	150	14.25	86.71	0.2	1.1	1.703	1.753	0.389	0.776*
5.63	0.8	45551	3005	15.16	87.48	1.7	5.6	0.314	0.324	0.074	0.976*

Table T5. Merging statistics of the other impurity in olanzapinium succinate (1:1) solved by MicroED

d_max	d_min	#obs	#uniq	mult.	%comp	<I>	<I/sI>	r_mrg	r_means	r_pim	cc1/2
5.89	2.14	3626	148	24.5	95.48	3.2	49.7	0.125	0.128	0.025	0.998*
2.14	1.71	4989	148	33.71	100	1.7	32.7	0.197	0.2	0.034	0.994*
1.71	1.5	5004	135	37.07	100	1.1	22.3	0.265	0.269	0.042	0.990*
1.5	1.36	5206	135	38.56	100	0.7	16.4	0.3	0.304	0.047	0.986*
1.36	1.27	4987	133	37.5	100	0.7	11.1	0.373	0.378	0.061	0.984*
1.27	1.19	5125	126	40.67	100	0.7	14.4	0.303	0.307	0.047	0.984*
1.19	1.13	5544	142	39.04	100	0.6	11.6	0.362	0.367	0.057	0.991*
1.13	1.08	4991	124	40.25	100	0.4	7.6	0.43	0.435	0.067	0.977*
1.08	1.04	5033	127	39.63	100	0.4	6.9	0.454	0.46	0.071	0.971*
1.04	1.01	5657	133	42.53	100	0.3	5.8	0.541	0.548	0.084	0.960*
1.01	0.98	4849	121	40.07	100	0.2	3.6	0.746	0.756	0.115	0.789*
0.98	0.95	5630	137	41.09	100	0.2	3	0.813	0.823	0.125	0.825*
0.95	0.92	5533	130	42.56	100	0.2	3.4	0.892	0.903	0.134	0.896*

0.92	0.9	4886	118	41.41	100	0.1	2.5	0.971	0.983	0.149	0.810*
0.9	0.88	5491	134	40.98	100	0.1	2.1	1.073	1.088	0.169	0.436*
0.88	0.86	5261	128	41.1	100	0.1	2.1	1.438	1.456	0.22	0.736*
0.86	0.84	5412	125	43.3	100	0.1	1.8	3.055	3.088	0.44	0.652*
0.84	0.83	5191	122	42.55	100	0.1	1.3	2.01	2.036	0.31	0.521*
0.83	0.81	5820	140	41.57	100	0.1	1.4	1.746	1.767	0.263	0.510*
0.81	0.8	4670	122	38.28	100	0.1	1.1	1.748	1.772	0.28	0.351*
5.89	0.8	102905	2628	39.16	99.73	0.6	10.6	0.384	0.389	0.061	0.995*

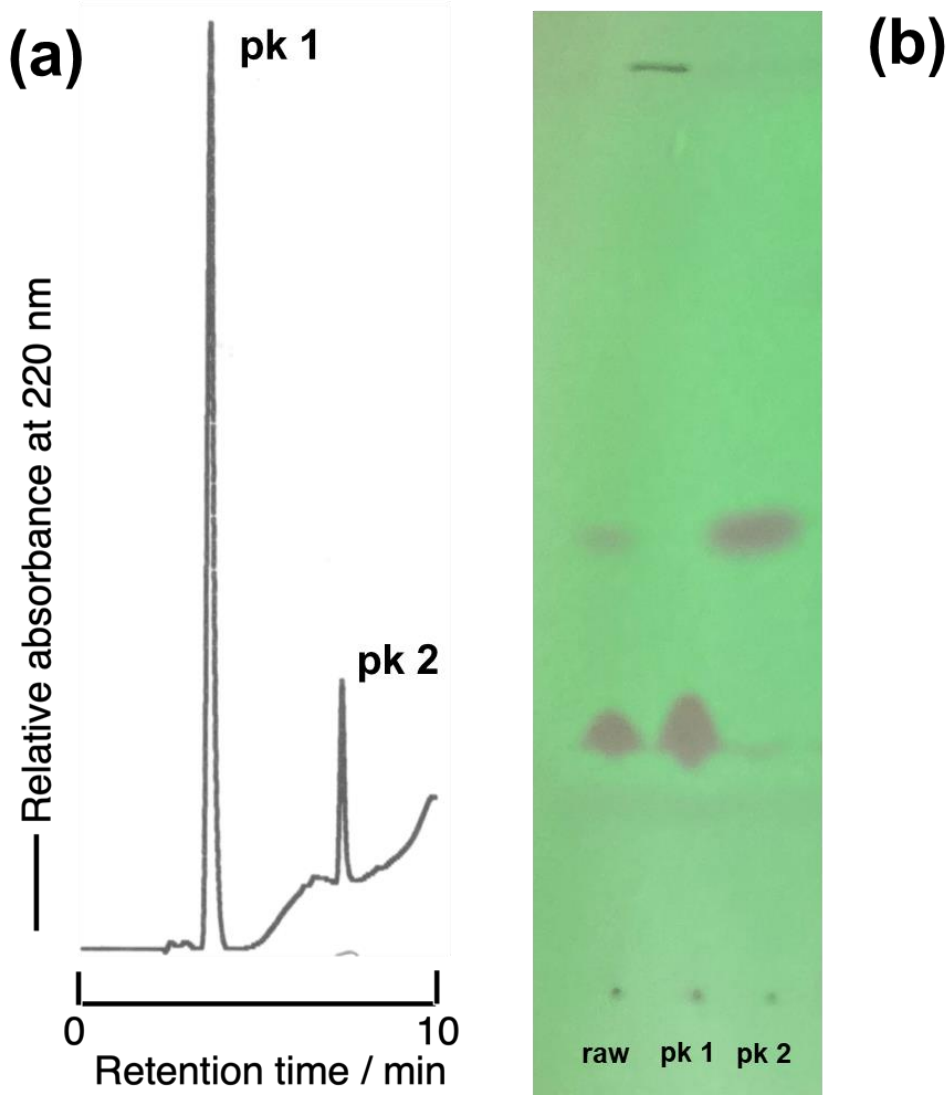

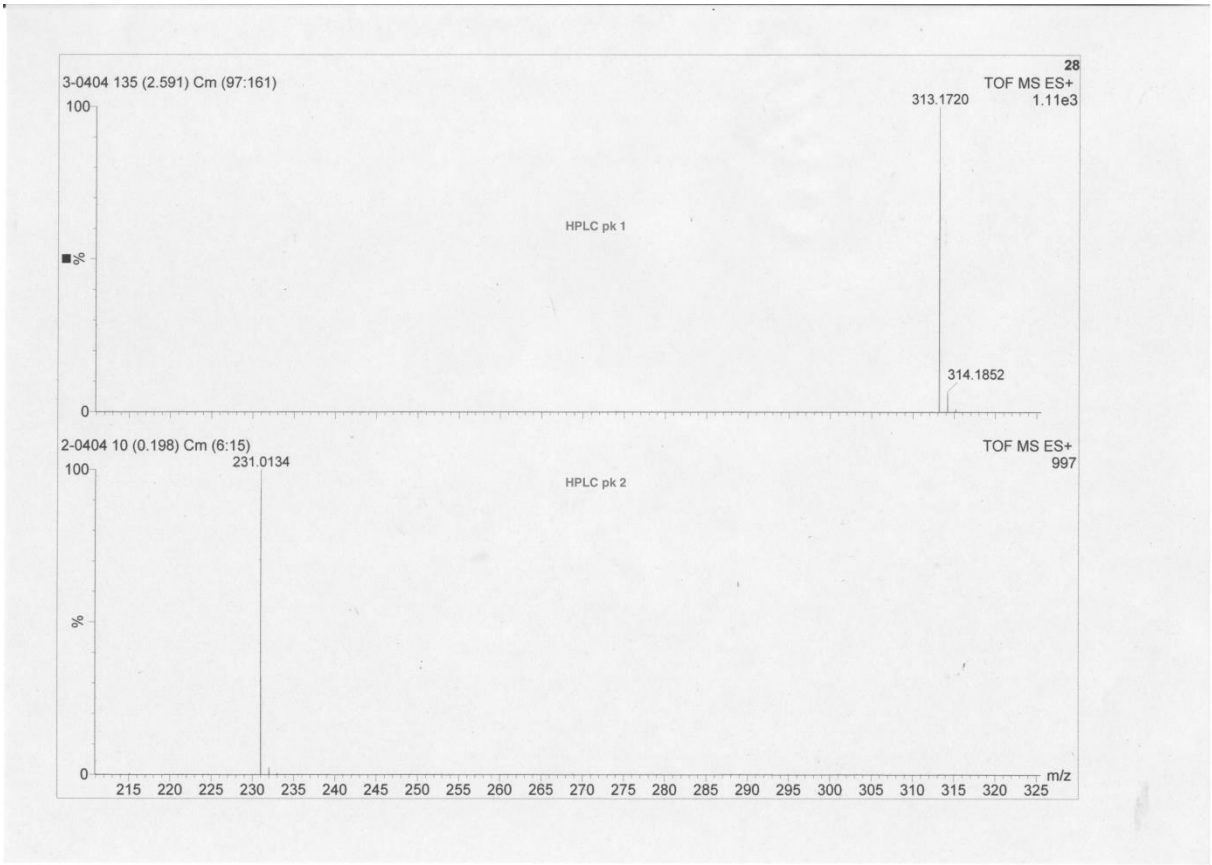

(c)

Figure S5. (a) HPLC and (b) TLC of the raw powder sample, that shows presence of OLN (pk 1), OLN fragment (pk2 also termed as OLN impurity 2) prior to MicroED data collection. TLC was developed from a solvent mixture of chloroform:methanol = 5:1 including 0.5% of triethylamine; (c) MS of the separated fragment using TLC showed presence of OLN (calculated for $C_{17}H_{20}N_4S$ $(M+H)^+$: 313.1487; found: 313.1720 (100%) and OLN fragment (calculated for $C_{12}H_{10}N_2OS$ $(M+H)^+$: 231.0592; found: 231.0134.